SUPPORTING INFORMATION

Diffusion of macromolecules in a polymer hydrogel: from microscopic to macroscopic scales

D. Sandrin, [1,*] D. Wagner, [2,*] C. E. Sitta, [3,*] R. Thoma, [4] S. Felekyan, [1] H. E. Hermes, [2] C. Janiak, [4] N. de Sousa Amadeu, [4] R. Kühnemuth, [1,†] H. Löwen, [3,‡] S. U. Egelhaaf, [2,§] C. A. M. Seidel [1,¶]

[1] *Institut für Physikalische Chemie II, Molekulare Physikalische Chemie,*

Heinrich-Heine-Universität, Universitätsstr. 1, 40225 Düsseldorf, Germany

[2] *Institut für Experimentelle Physik der kondensierten Materie,*

Heinrich-Heine-Universität, Universitätsstr. 1, 40225 Düsseldorf, Germany

[3] *Institut für Theoretische Physik II: Weiche Materie,*

Heinrich-Heine-Universität, Universitätsstr. 1, 40225 Düsseldorf, Germany

[4] *Institut für Anorganische Chemie und Strukturchemie,*

Heinrich-Heine-Universität, Universitätsstr. 1, 40225 Düsseldorf, Germany

(Dated: February 26, 2016)

*these authors have contributed equally to this work

† ralf.kuehnemuth@hhu.de; corresponding author

‡ hlowen@hhu.de; corresponding author

§ stefan.egelhaaf@hhu.de; corresponding author

¶ cseidel@hhu.de; corresponding author

Materials and Methods

S1. *Dextran samples & hydrogel – fluorescence properties and quantitative FCS*

S1.1. *Manufacturers details of fluorescent samples*

Samples	Degree of labelling	Number of lysines	Number of amines[(a)]	Charge[(b)]	Absorption Max [nm]	Emission Max [nm]	Quantum yield[(c)]
A488-D3	1	0	≥ 1	a	495	517	0.6
A488-D10	1	10	≥ 2.5	a	494	516	0.6
FLU-D3	1	0	≥ 1	a	497	523	0.5
FLU-D10	2	0	≥ 2.5	a	496	521	0.5
FLU-D40	5	0	≥ 5	a	496	521	0.5
FLU-D500	86	58	≥ 50	a	496	521	0.2
TMR-D3	1	0	≥ 1	a	560	584	0.7
TMR-D10	3	0	≥ 2.5	n	559	586	0.5
TMR-D40	8	0	≥ 5	n	560	586	0.6
TMR-D70	10	0	≥ 10	n	560	585	1
TMR-D2000	138	456	not specified	not specified	560	583	0.8

Table S1. The table shows the manufacturers specification of dye-labelled dextran conjugates (data sheets of used sample batches, Invitrogen). [(a)] Specified for unlabelled aminodextrans. [(b)] a: anionic, n: neutral. [(c)] Fluorescence quantum yield Φ_F determined relative to fluorescein at pH 8.0 (FLU and A488; $\Phi_F^{\mathrm{FLU}} = 0.925 \pm 0.015$ [1]) or relative to 5-(and-6)-carboxytetramethylrhodamine (TMR).

S1.2. *Investigation of partial quenching (quantum yield and fluorescence lifetime)*:

For the sample A488-D10 the partial quenching of the labels as indicated in table S1 was investigated applying time-correlated single photon counting (TCSPC, table S2).

fl. lifetime (species fraction)	τ_1 [ns] (x_1)	τ_2 [ns] (x_2)	τ_3 [ns] (x_3)	τ_4 [ns] (x_4)	τ_5 [ns] (x_5)	χ^2	τ_x [ns]
A488 / H_2O	4.125 (0.978)	0.459 (0.022)	/	/	/	1.13	4.045
A488-D10 / H_2O	4.125 (0.742)	2.459 (0.104)	0.932 (0.066)	0.260 (0.089)	/	1.30	3.400
A488-D10 / H_2O (corr.)	4.125 (0.548)	2.459 (0.077)	0.932 (0.049)	0.260 (0.065)	0 (0.262)	1.30	2.511

Table S2. Lifetime components of A488 and A488-D10 in H_2O (FT300, PicoQuant, Berlin; excitation: 485 nm, emission: 517-523 nm, magic angle, photons recorded: total 5×10^8, peak channel 10^6 photons, T=20 °C). τ_x: species averaged fluorescence lifetime.

While free A488 decays almost mono-exponentially its D10-conjugate exhibits at least four lifetime components, indicating dynamic quenching of a subset of the labels. Albeit, the obtained species averaged lifetimes, $\tau_x = \sum x_i \tau_i$, of conjugated and free dye are not consistent with the determined corresponding fluorescence quantum yields, Φ_F. According to the ratio of the quantum yields of the labelled dextran ($\Phi_F^{\mathrm{A488-D10(exp)}} = 0.57$, measured versus Rhodamine 110, $\Phi_F^{\mathrm{Rh110}} = 0.85$,[2] consistent with manufacturers information $\Phi_F^{\mathrm{A488-D10(man)}} = 0.6 \times 0.925 = 0.56$) and the A488 dye free in aqueous solution ($\Phi_F^{\mathrm{A488}} = 0.92$, Invitrogen online) a ratio of the species averaged fluorescence lifetimes of $\tau_x^{\mathrm{A488-D10}} / \tau_x^{\mathrm{A488}} \equiv \Phi_F^{\mathrm{A488-D10}} / \Phi_F^{\mathrm{A488}} = 0.57/0.92 = 0.62$ is expected. Thus a fraction of completely (statically) quenched labels of x_5 = 0.262 can be deduced (last row in table S2; $\tau_x^{\mathrm{A488-D10,corr}} / \tau_x^{\mathrm{A488}} = 2.511/4.045 = 0.62$). The resulting unquenched fraction then is $x_1^{\mathrm{A488-D10}} / x_1^{\mathrm{A488}} = 0.560$ and the remaining fraction of $1 - 0.560 - 0.262 = 0.179$ represents the partially (=dynamically) quenched dyes. For sake of simplicity, in the following the partially quenched fraction will be ignored and instead an effective totally quenched portion of x_q = 0.38 and a corresponding fluorescent portion of x_f = 1- x_q = 0.62 will be assumed.

S1.3. *The effective degree of labelling* ($DoL_{\text{eff.}}$):

The fluorescently labelled dextrans (as provided by Invitrogen, their specifications being summarized in table S1) are produced by exposing aminodextrans with an average number n_a of free amino groups to amine-reactive dye conjugates. Except for the A488 conjugates, once the dye has been added, the unreacted amines on the dextran are capped to yield a neutral or anionic dextran. Some of the samples carry additional lysines. Due to the applied labelling procedure, for any average degree of labelling, DoL_{av}, a distribution, $P(n_d)$, of the number of dyes per dextran molecule, n_{d}, is anticipated, i.e. even samples with a $DoL_{\text{av}} = 1$ will contain unlabelled as well as higher $(n_a \geq n_d > 1)$ labelled molecules. In case of random labelling, the distribution of n_{d} can be approximated by the binomial distribution:

$$P(n_d, n_a, DoL_{av}) = \frac{n_a!}{n_d!(n_a - n_d)!}\left(\frac{DoL_{av}}{n_a}\right)^{n_d}\left(1 - \frac{DoL_{av}}{n_a}\right)^{n_a - n_d} \qquad \text{(S1)}$$

For many labelled dextrans the fluorescence quantum yield is significantly reduced as compared to the free dye. Assuming only static quenching of the dyes (on the time scale of the experiment) three different distributions can be defined: (1) the distribution of dextrans $P(n_t)$ containing any number n_t of dyes (fluorescent or quenched) in the range of $n_a \geq n_t \geq 0$, (2) the distribution of dextrans $P(n_f)$ carrying n_f fluorescent (non-quenched) dyes, and (3) the distribution of dextrans containing any dye (fluorescent or quenched) under the condition that at least one fluorescent dye is present, $P(n_{t(f)})$. While $P(n_t) = P(n_d)$, $P(n_f)$ can easily be obtained from eq. S1 by replacing DoL_{av} with $DoL_{\text{av}} \times x_f$. The fluorescent fraction of the dyes x_f is approximated by the relative quantum yield of the labelled dextran as compared to the corresponding free dye, $x_f = \Phi_F^{\text{dextran}} / \Phi_F^{\text{free dye}}$ (see S1.2). The third distribution, $P(n_{t(f)})$, is obtained for $n_a \geq n_{t(f)} > 0$ from $P(n_t)$ by randomly distributing quenched dyes among the labelled dextrans, i.e. multiplying a second binomial distribution with $P(n_t)$ and adding the probabilities for all species with the same n_t that contain at least one fluorescent label. The unlabelled fraction is $P(n_{t(f)} = 0) = P(n_f = 0)$.

By omitting the corresponding unlabelled fractions ($n_t = 0$, $n_f = 0$ or $n_{t(f)} = 0$, respectively), three different effective degrees of labelling, DoL_{eff}^{x}, can be calculated from the obtained distributions using eq. S2:

$$DoL_{eff}^{x} = \sum_{n_x=1}^{n_a} n_x P(n_x) \Big/ \sum_{n_x=1}^{n_a} P(n_x) \qquad \text{(S2)}$$

with $x = t, f$ or $t(f)$, as defined above.

For A488-D10, the sample investigated in greatest detail in the current study, this will be shown in the following (table S3). For this sample $DoL_{av} = 1$ as determined by the manufacturer and $x_f = 0.62$ for the fluorescent fraction of the labels (see lifetime analysis S1.2) was assumed. Since the number of initial amino groups (n_a) per dextran could not be obtained from the manufacturer an average number of n_a=5 was estimated (being the mean $<n_a>$ for the currently available 18 batches of unlabelled aminodextrans D10 as specified on the manufacturers homepage). Choosing n_a=4 or n_a=6 does not significantly change the following considerations.

n_x	0	1	2	3	4	5	DoL^x_{eff}	x_f
$P(n_t)$	0.328	0.410	0.205	0.051	0.006	3×10^{-4}	1.49	1
$P(n_f)$	0.515	0.365	0.104	0.015	0.001	3×10^{-5}	1.28	0.62
$P(n_{t(f)})$	0.515	0.254	0.175	0.048	0.006	0.003	1.60	0.62

Table S3. Expected distribution of probabilities of labelled dextrans D10 ($P(n_t)$) assuming random labelling and a binomial distribution of the labels number, n_t, as well as corresponding distributions taking the fluorophores partial static quenching into account ($P(n_f)$ and $P(n_{t(f)})$. DoL_{av}=1, available labelling sites n_a=5. x_f is the fluorescent (non-quenched) fraction of the dyes. DoL^x_{eff} with $x = t, f, t(f)$ are the effective degrees of labelling considering all labels and labelled dextrans, only fluorescent labels and fluorescently labelled dextrans and all labels but only fluorescent dextrans, respectively.

The estimation of $DoL^{t(f)}_{eff}$ assumed only static quenching for the partially quenched sample and thus presents a border case, but can be justified by the fact that, according to fluorescence lifetime analysis, the fraction of completely quenched dyes significantly exceeds the dynamically quenched portion (26% vs. 18%). The distribution of the total number of labels ($P(n_t)$ or $P(n_{t(f)})$) is relevant for the estimation of average ionic charges carried by the label. Here $P(n_{t(f)})$ yields the higher number of the two but might be an overestimation, since partial quenching of the individual fluorophores was excluded. Thus the true value of $DoL^{t(f)}_{eff}$ as required to estimate the molecular charge due to labelling is expected to be in between the lower and upper limits as calculated via $P(n_t)$ and $P(n_{t(f)})$, respectively.

The distribution of fluorescent labels, $P(n_f)$, has implications on the molecular brightness as observed by FCS as will be shown in S1.4.

S1.4. *Implications of the distribution of molecular brightnesses for quantitative FCS*:

In FCS the molecular brightness B is estimated by dividing the detected fluorescence count rate F by the observed number of fluorescent molecules, N_{tot}, simultaneously present in the confocal detection volume element, $B = F/N_{tot}$. In case of identical brightness of all particles N_{tot} can directly be obtained from the amplitude of the correlation function (eq. 4 main document, $N_{tot}=N$ for negligible triplet population). A distribution of brightnesses as discussed above would increase the observed amplitude, i.e. yielding an apparent (or effective) number of molecules N_{eff} (eq. S3).[3]

$$N_{eff} = N_{tot}\left(\sum_{n_f} n_f P(n_f)\right)^2 \Big/ \sum_{n_f} n_f^2 P(n_f) \qquad \text{(S3)}$$

Applying eq. S3 to the numbers in the table S3 yields $N_{eff}=0.856\ N_{tot}$. With $DoL_{eff,\ f.}=1.28$ an effective molecular brightness $B^{A488\text{-}D10}/B^{A488}=1.28/0.856=1.5$ is predicted and fully confirmed by experiment ($B^{A488\text{-}D10}\approx 6.8$ kHz/molecule, $B^{A488}\approx 4.5$ kHz/molecule; → $B^{A488\text{-}D10}/B^{A488}=1.5$). Ignoring the distribution of labels would falsify the determined molecular concentrations by almost 15 % and the corresponding brightnesses by 50 %. To derive the total number of dextran molecules, N_{dex}, in the confocal volume in addition the non-fluorescent labels portion needs to be considered ($P(n_f=0)$ = 0.515, table SI 3): $N_{dex}=N_{eff}\cdot(0.856)^{-1}\times(1\text{-}0.515)^{-1}=2.41\cdot N_{eff}$. Comparing the concentrations of a series of A488-D10/H_2O solutions (not shown) as determined by FCS (confocal detection volume element $V_{det}=0.55$ fl) and its extinction (71,000 $cm^{-1}M^{-1}$ at 496 nm, Invitrogen) we find $N_{dex}(exp)=2.9\ N_{eff}$, consistent with the estimated number within the anticipated uncertainties of the confocal volume determination (±15 %), the measured quantum yield (± 10 %), the average degree of labelling (manufacturers specification) and the approximations made by calculating the dye distributions.

The experimental confirmation of the estimated effective brightness justifies the assumption made above of a random distribution of the quenched labels. An alternative scenario, e.g. quenching due to dye-dye interaction, might be indicated by the similarity of the estimated portion of the singly labelled dextrans ($P(n_t=1)=0.41$, corresponding to 61 % of the labelled molecules) and the fraction of unquenched dye as determined by TCSPC (56 %). This would lead to an expected effective molecular brightness of the dextran A488-D10 close to the free dye brightness and is not consistent with our FCS results.

S1.5. *Effect of immobile fluorophores on molecular brightness in FCS*:

In a stationary confocal measurement, i.e. keeping the location of the confocal volume fixed, the number of fluorophores that are immobile on the time scale of the experiment, N_{immob}, will not contribute to fluctuations of the fluorescence, provided temporary dark state population is negligible. In that case their fluorescence, F_{immob}, can be considered like uncorrelated background. This would reduce the correlation amplitude, $1/N_{\mathrm{mob}}$ (the inverse number of diffusing fluorescent particles) corresponding to the fluorescence, F_{mob}, of mobile fluorophores and yield an apparent amplitude, $1/N_{\mathrm{app}}$[3].

$$N_{mob} = N_{app}\left(\frac{F_{mob}}{F_{mob}+F_{immob}}\right)^2 = N_{app}\left(\frac{F_{mob}}{F_{tot}}\right)^2 \tag{S4}$$

$F_{\mathrm{tot}}=F_{\mathrm{mob}}+F_{\mathrm{immob}}$ is the total fluorescence, $N_{\mathrm{tot}}=N_{\mathrm{mob}}+N_{\mathrm{immob}}$ the total number of fluorescent particles. For brightness $B_{\mathrm{mob}}=B$ of mobile and $B_{\mathrm{immob}}=n_{\mathrm{i}}B$ of immobile particles follows (with $n_{\mathrm{i}}>0$):

$$N_{mob} = N_{app}\left(\frac{N_{mob}}{N_F}\right)^2 = N_{app}\left(\frac{N_{mob}}{N_{mob}+n_i N_{immob}}\right)^2 = N_{app}\left(\frac{N_{mob}}{n_i N_{tot}-(n_i-1)N_{mob}}\right)^2.$$

Here N_{F} is the equivalent total number of fluorophores with brightness B. With the apparent brightness $B_{app}=\frac{F_{tot}}{N_{app}}$ we get

$$B = \frac{F_{mob}}{N_{mob}} = \frac{F_{tot}}{n_i N_{tot}-(n_i-1)N_{mob}} = B_{app}\frac{N_{app}}{n_i N_{tot}-(n_i-1)N_{mob}} \quad \text{and}$$

$$N_{mob} = N_{app}\left(\frac{B_{app}}{B}\right)^2$$

$$n_i N_{tot}-(n_i-1)N_{mob} = N_{app}\frac{B_{app}}{B} = \frac{F_{tot}}{B}$$

$$\Rightarrow \frac{n_i N_{tot}-(n_i-1)N_{mob}}{N_{mob}} = \frac{B}{B_{app}} = \frac{n_i N_{tot}}{N_{mob}}-(n_i-1) \tag{S5}$$

$$\Rightarrow x_{mob} = \frac{N_{mob}}{N_{tot}} = n_i\left(\frac{B}{B_{app}}+n_i-1\right)^{-1} = 1-x_{immob}$$

Provided translational diffusion is the only process leading to fluorescence fluctuations, e.g. for $n_{\mathrm{i}}=1$ (identical brightness), the mobile fraction can easily be obtained from $x_{\mathrm{mob}}=N_{\mathrm{mob}}/N_{\mathrm{tot}}=B_{\mathrm{app}}/B$. Thus the apparent change in molecular brightness as determined by stationary FCS can give information about the portion of mobile species otherwise invisible to this method.

For the samples studied, in particular the A488-D10, only a minor change in fluorescence lifetime due to quenching upon entering the hydrogel was observed ($\tau_{gel}/\tau_{sol}\approx0.97$, approximately half of the effect being caused by refractive index changes. See main document and S1.6), suggesting that the average molecular brightness in a first approximation can be considered as unaffected by the hydrogel. From FCS investigations of different concentrations of A488-D10/H_2O in the hydrogel between 30 and 100 nM we obtained an apparent molecular brightness of $B_{app}\approx2.5$ kHz/molecule. With $B\approx6.8$ kHz/molecule as measured free in solution a completely immobile fraction of $x_{immob}\approx0.63$ would have to be concluded from eq. S5. Since higher labelled molecules are preferentially trapped (see main document) this must be considered as an upper limit. In case all immobile particles were doubly labelled and the mobile ones would carry one fluorophore ($B_{mob}=B^{A488}=4.5$ kHz/molecule$=0.5B_{immob}$) an estimation according to the above analysis would yield $x_{mob}=2/((B/B_{app})+1)$ and $x_{immob}\approx0.29$. This is higher than the estimated fraction of A488-D10 with $n_f>1$ (12 %, table S3) and could indicate an enrichment of higher labelled dextrans inside the hydrogel, consistent with the observation of a higher binding constant for those probe molecules (main document).

S1.6. *Refractive index mismatch – effect on fluorescence lifetime and diffusion measurements*:

Inside the PAAm hydrogel the refractive index, n, is reported to be slightly higher than in dilute aqueous solutions.[4] For the densities of hydrogels and the wavelength used in our study a linear dependence of $dn/dc'=0.188$ ml/g can be extracted, with c' being the mass of PAAm per ml hydrogel. With $n_0=1.3361$ for water ($\lambda=525$ nm and T=22 °C)[5] and the measured densities of the gels (see main document, converted using a density of $\rho_{(PAA)}=1.3$ g/cm^3) we estimate the refractive indices in table S4.

Based on the refractive index, changes in radiative lifetimes, τ_r, can be calculated according to Toptygin by a modified Strickler-Berg approach.[6] The empty spherical cavity model (ESC, Toptygin, eq. 59) was found to successfully describe radiative lifetimes of small fluorophores in solution (eq. S1.5):

$$\frac{\tau_{r,2}}{\tau_{r,1}}=\left(\frac{n_1}{n_2}\right)^5\left(\frac{2n_2^2+1}{2n_1^2+1}\right)^2 \qquad \text{(S6)}$$

$\tau_{r,1}$ and n_1 are radiative lifetime and index of refraction in water, $\tau_{r,2}$ and n_2 the corresponding quantities in the gel (table S.4).

hydrogel	c [ml/ml]	c' [g/ml]	n	$\tau_{r(gel)}/\tau_{r(sol)}$
pH7	0.038	0.049	1.3454	0.987
ph10	0.015	0.020	1.3398	0.995

Table S4. Index of refraction at λ=525 nm and T=22 °C for PAAm hydrogels and its estimated effect on radiative lifetimes.

For A488 and A488-D10 the observed changes in fluorescence lifetimes are bigger than the predicted changes in radiative lifetime, suggesting additional fluorescence quenching due to matrix effects (see main document).

The relative small deviation of n from n_0 (H_2O) is well within the range of the correction collar of current water immersion objectives. This was shown for a Zeiss CApo40x/1.2 W objective,[7] comparable to our Olympus UPlanSApo 60x/1.2 W, and verified by experiment. Furthermore, in a calibration measurement we confirmed that for our conditions (wavelength, depth of the focal point in the sample) no readjustment of the correction collar setting was required after switching the sample from pure water to hydrogel.

S1.7. Binding model

A simple binding model was applied to describe the observed equilibrium fractions of mobile and trapped probe molecules:

$$\begin{aligned} K_d &= \frac{a_{bound}}{a_{free} \cdot a_{sites}} \\ K_d' &\approx K_d \cdot a_{sites} = \frac{a_{bound}}{a_{free}} \approx \frac{c_{bound}}{f_{free} c_{free}} \\ &\Rightarrow \frac{c_{bound}}{c_{free}} = f_{free} K_d' \\ &\Rightarrow \frac{c_{bound}}{c_{free} + c_{bound}} = x_{bound} = \frac{f_{free} K_d'}{1 + f_{free} K_d'} \end{aligned} \tag{S7}$$

Here, K_d is the binding constant, a the activity for free (a_{free}) and bound (a_{bound}) molecules with the respective concentration (c_{bound} and c_{free}). The number of binding sites in the matrix a_{sites} defines the effective binding constant K_d'.

Results

S2. *Image integrated normalized correlations curves measured in hydrogel for A488-Dx and TMR-Dx in water and for FLU-Dx in carbonate buffer 20 mM pH 10*

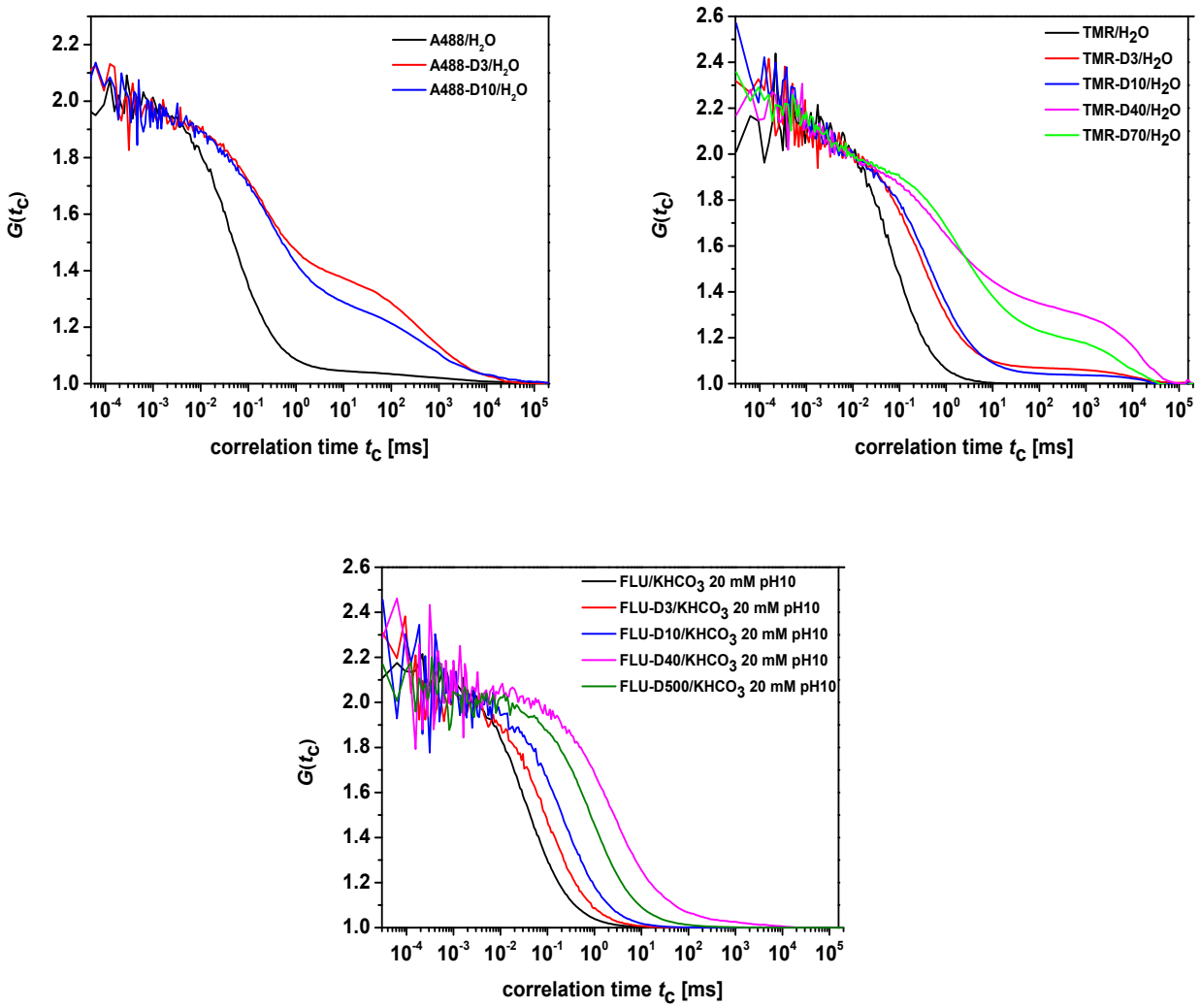

Figure S1. Image integrated normalized correlations curves for A488 and TMR free dye and with dextran in hydrogel in water conditions. In this case, more than one diffusion time is clearly visible, indicating the presence of temporarily trapped molecules in the hydrogel. FLU samples were measured in carbonate buffer 20 mM, pH 10, in this case the bound molecules are much less, only for samples D40 and D500 trapping is visible and amounts to about 1%.

S3. *Diffusion times from FCS experiments in the hydrogel at standard conditions*

Table S5 shows the diffusion times for A488, TMR and FLU for free dye and with dextran at standard conditions: water for A488 and TMR, carbonate buffer pH 10 for FLU in the hydrogel.

Dye	**Sample**	**Solvent**	**fast component**		**slow component**	
			t_d **[ms]**	**fraction x**	t_d **[ms]**	**fraction x**
A488	Free dye	H_2O	0.049 ± 0.002	0.991	200-500	0.009
A488	D3	H_2O	0.220 ± 0.007	0.626	10-2000	0.374
A488	D10	H_2O	0.410 ± 0.017	0.704	10-6000	0.296
TMR	Free dye	H_2O	0.065 ± 0.001	1	-	0
TMR	D3	H_2O	0.272 ± 0.010	0.873	10-8000	0.127
TMR	D10	H_2O	0.363 ± 0.011	0.962	1000-10000	0.038
TMR	D40	H_2O	1.699 ± 0.105	0.688	20-10000	0.312
TMR	D70	H_2O	2.026 ± 0.079	0.719	40-12000	0.281
FLU	Free dye	$KHCO_3$ 20 mM pH 10	0.036 ± 0.001	1	-	0
FLU	D3	$KHCO_3$ 20 mM pH 10	0.116 ± 0.001	1	-	0
FLU	D10	$KHCO_3$ 20 mM pH 10	0.263 ± 0.004	1	-	0
FLU	D40	$KHCO_3$ 20 mM pH 10	0.823 ± 0.032	0.992	10-140	0.008
FLU	D500	$KHCO_3$ 20 mM pH 10	3.664 ± 0.470	0.988	20-3000	0.012

Table S5. Results of FCS fits for A488, TMR and FLU (free dye and labelled dextran) in hydrogel. For some samples fitting the model function to the data required two or more diffusion times. In the latter case the fraction of the slow component (last column) is the sum of two terms that in total represent the fraction of trapped molecules. The diffusion times of fast components are the averages from different pixels. For the slow component, t_d is given as range because it significantly differs from pixel to pixel.

S4. *Diffusion times from FCS experiments for Rh110, A488, TMR and FLU free dye and labelled D10 at different salt conditions in the hydrogel.*

Sample	Solvent	fast component		slow component	
		t_d [ms]	fraction x	t_d [ms]	fraction x
Rh110	H_2O	0.036	1	-	0
A488	H_2O	0.049	0.991	200-500	0.009
A488-D10	H_2O	0.410	0.704	10-6000	0.296
A488-D10	$KClO_4$ 10 mM	0.384	0.832	10-6000	0.168
A488-D10	$KClO_4$ 20 mM	0.383	0.875	10-6000	0.125
A488-D10	KCl 20 mM	0.352	0.904	400-6000	0.096
A488-D10	$KClO_4$ 40 mM	0.401	0.900	10-6000	0.100
A488-D10	$KClO_4$ 60 mM	0.352	0.910	10-6000	0.090
A488-D10	$KHCO_3$ 20 mM pH 7	0.345	0.924	400-6000	0.076
A488-D10	$KHCO_3$ 20 mM pH 10	0.354	0.930	400-6000	0.070
TMR-D10	H_2O	0.363	0.960	500-7000	0.040
TMR-D10	$KHCO_3$ 20 mM pH 10	0.303	1	-	0
TMR-D10	TRIS 50 mM pH 7.5	0.212	1	-	0
FLU-D10	$KHCO_3$ 20 mM pH 10	0.265	1	-	0
FLU-D10	H_2O	0.260	1	-	0
FLU-D10	TRIS 50 mM pH 7.5	0.262	1	-	0

Table S6. Results of FCS fits for the reference Rh110, A488, A488-D10, TMR-D10 and FLU-D10 in solution and in the hydrogel at different salt conditions. For some samples fitting the model function to the data required two or more diffusion times. In the latter case the fraction of the slow component (last column) is the sum of two terms that in total represent the fraction of trapped molecules. The diffusion times of the fast components are the averages obtained from different pixels. For the slow component, t_d is given as range because it significantly differs from pixel to pixel.

S5. *Trace analysis*

The fluorescence time trace was split into small segments and sorted according to their approximated mean count rate employing a special feature of the binary single photon data format *.ht3 (PicoQuant, Berlin, Germany). Depending on the inter-photon time (i.e. the inverse count rate) in addition to the photon information extra entries are generated to store each overflow of the macroscopic time counter. Thus, sections containing the same total number of entries (as were generated upon splitting the recorded file) can be sorted by their content of photons and extra entries and thereby by their mean count rate. The produced subsets of split files were subsequently correlated and analyzed.

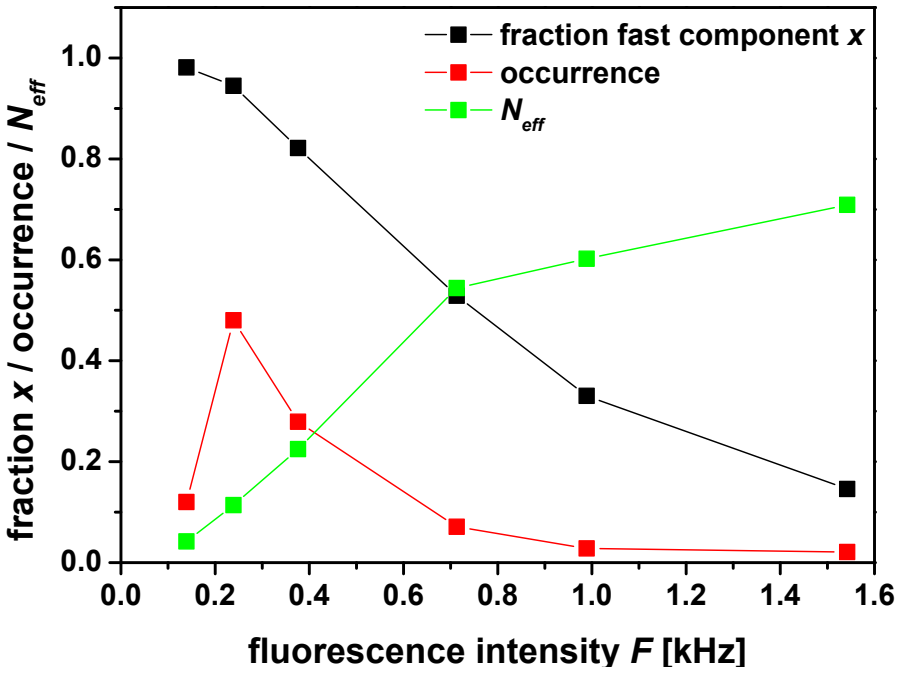

Figure S2. Fraction of fast component x, effective mean fluorophore number N_{eff} and occurrence of different count-rate based sections in time trace (Main document Figure 4). N_{eff} is the inverse correlation amplitude at τ_c=0 and corresponds to the total number of diffusing molecules in case of equal brightness for all components. Temporary accumulation of particles due to trapping is clearly visible.

S6. *Fluorescence intensity ratio between gel and the solution surrounding the gel plotted against experimental concentration for A488-D10 in H_2O from FCS measurements*

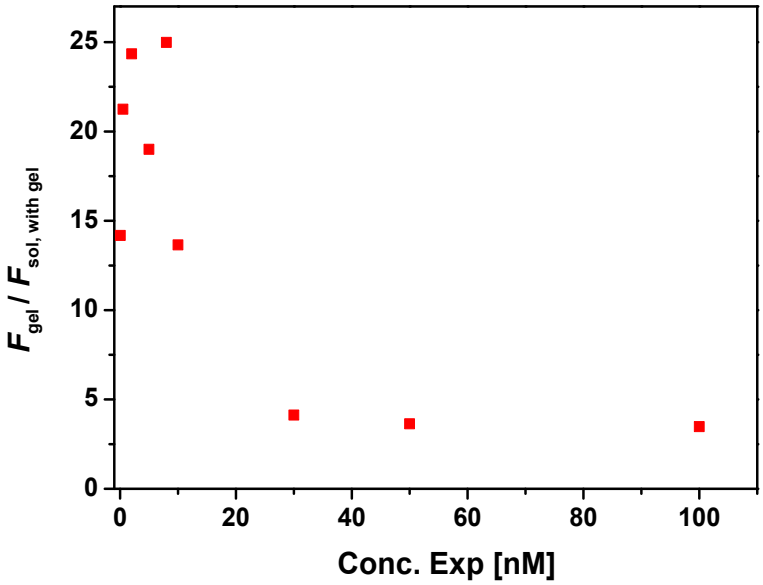

Figure S3. The plot shows that the fluorescence intensity ratio between gel and the solution surrounding the gel, F_{gel} / $F_{sol\ with\ gel}$, is decreasing with increasing experimental concentration. The enrichment of the fluorophores inside the gel, as indicated by the fluorescence intensity ratio is concentration dependent and strongest for small concentrations until high-affinity trap sites are saturated.

S7. *Fluorescence anisotropies of A488-D10, TMR-D10 and FLU-D10 in solution and hydrogel*

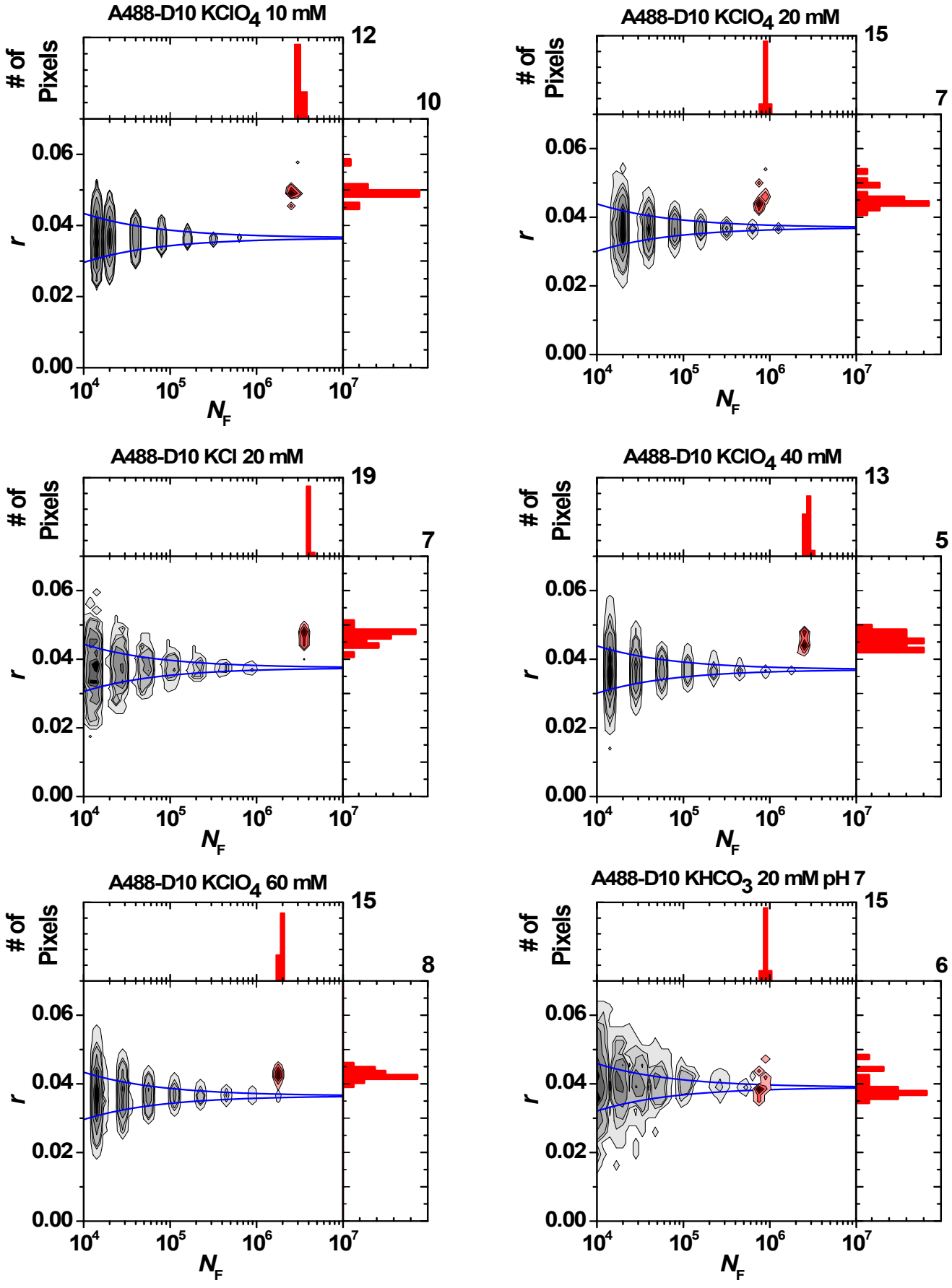

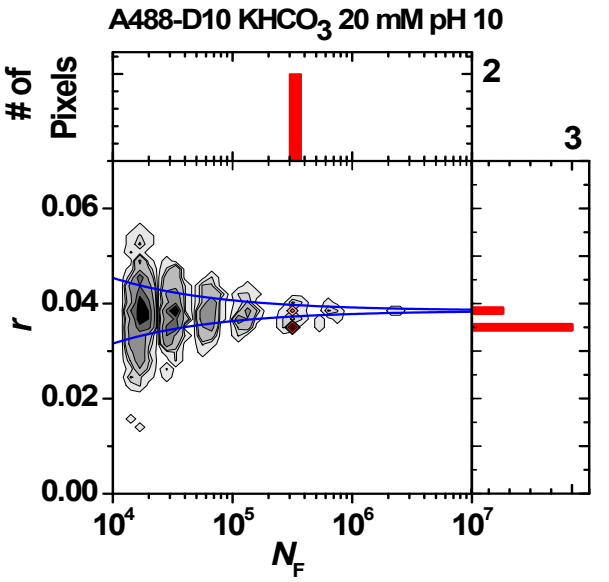
A488-D10 KHCO3 20 mM pH 10
# of Pixels
2
3
0.06
0.04
0.02
0.00
r
10^4
10^5
10^6
10^7
N_F

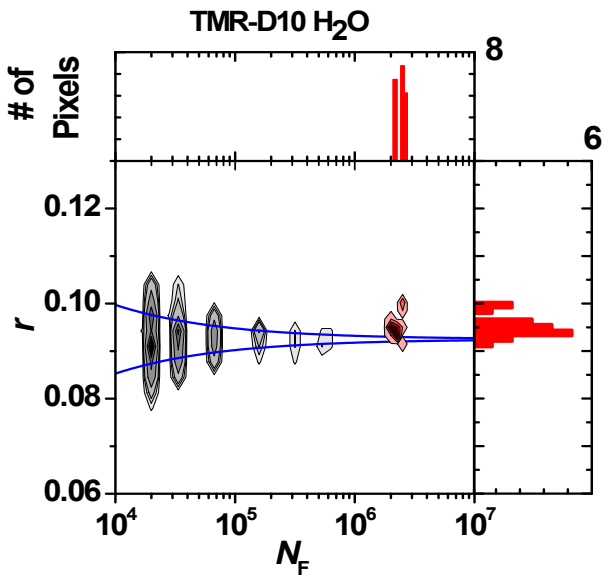
TMR-D10 H2O
# of Pixels
8
6
0.12
0.10
0.08
0.06
r
10^4
10^5
10^6
10^7
N_F

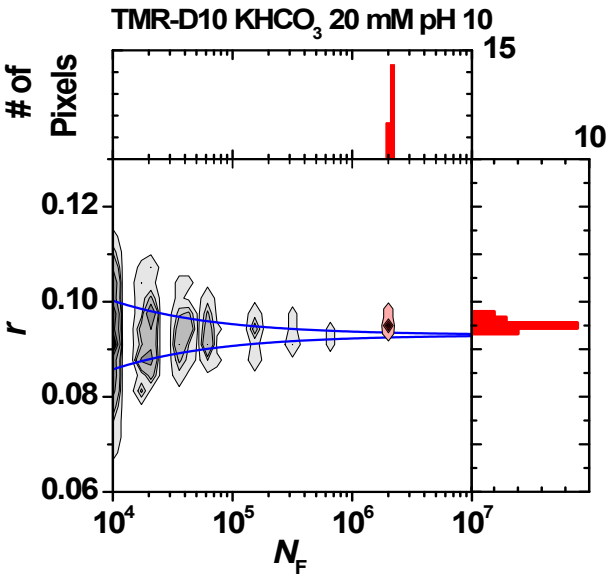
TMR-D10 KHCO3 20 mM pH 10
# of Pixels
15
10
0.12
0.10
0.08
0.06
r
10^4
10^5
10^6
10^7
N_F

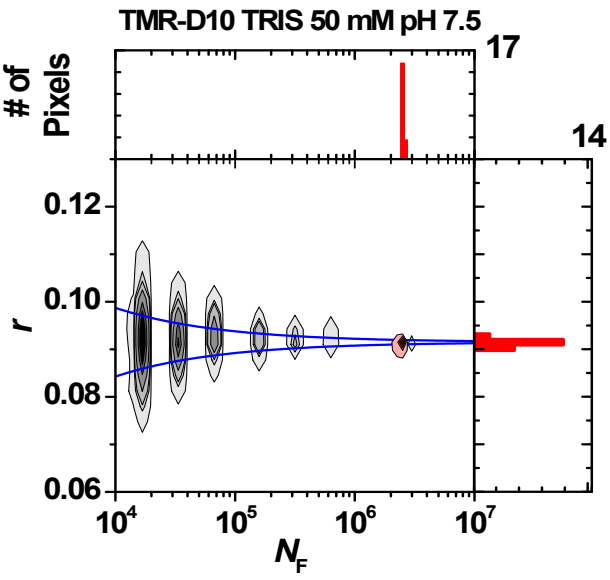
TMR-D10 TRIS 50 mM pH 7.5
# of Pixels
17
14
0.12
0.10
0.08
0.06
r
10^4
10^5
10^6
10^7
N_F

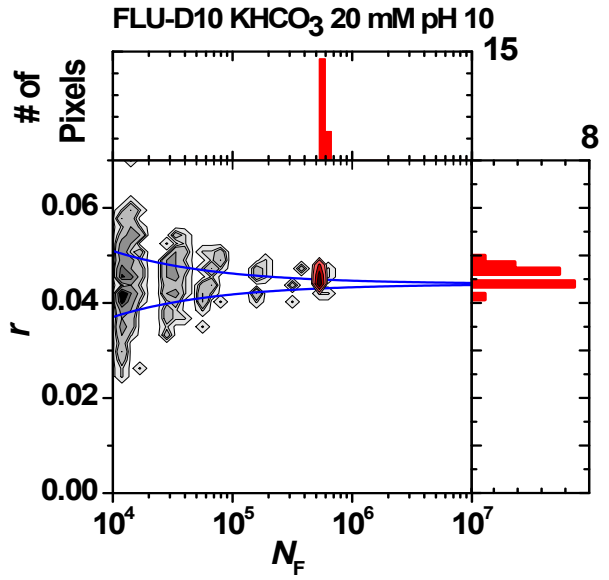
FLU-D10 KHCO3 20 mM pH 10
# of Pixels
15
8
0.06
0.04
0.02
0.00
r
10^4
10^5
10^6
10^7
N_F

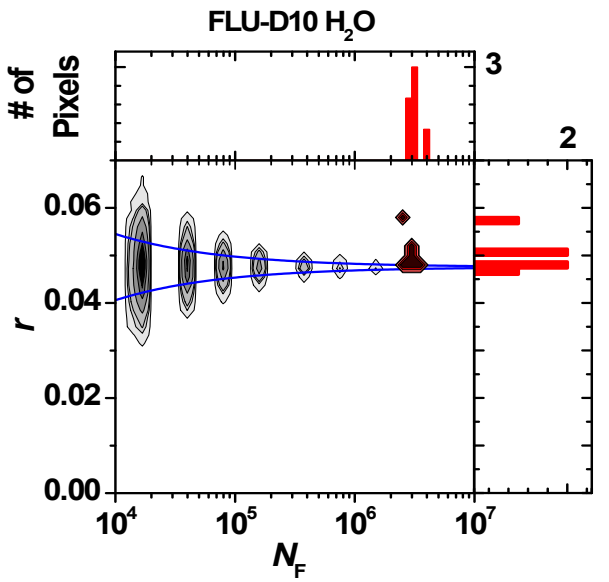
FLU-D10 H2O
# of Pixels
3
2
0.06
0.04
0.02
0.00
r
10^4
10^5
10^6
10^7
N_F

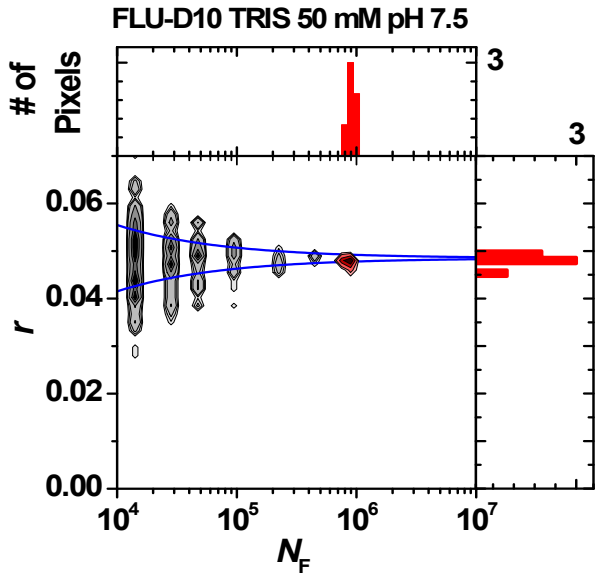

Figure S4. 2D plots of anisotropy *r* vs. photon number N_F for A488-D10, TMR-D10 and FLU-D10 in solution (gray contour lines) and in hydrogel (red contour lines) with 1D projections for the gel data.

For A488-D10 the plots show markedly different anisotropies inside the hydrogel for different solvent conditions. In case of $KClO_4$ 10 mM, 20 mM, 40 mM and KCl 20 mM the anisotropy in the gel is higher as compared to the solution value, in these cases the trapped fraction is≥10 %. The decrease in anisotropy starts with higher ionic strength: 60 mM $KClO_4$ and 20 mM in carbonate buffer pH 7 and 10, clearly correlated with the trapped fraction of the molecules as determined by FCS. For TMR-D10 and FLU-D10 the anisotropy is slightly higher or equal in comparison to solution measurements in different conditions (trapped fraction≤4%).

S8. *Fluorescence anisotropy A488-D10, TMR-D10 and FLU-D10*

Sample	Solvent	*r*		Trapped fraction
		Solution	Hydrogel	x
Rh110	H_2O	0.010	0.010	0
A488	H_2O	0.014	0.018	0.011
A488-D10	H_2O	0.037	0.049	0.296
A488-D10	$KClO_4$ 10 mM	0.037	0.049	0.168
A488-D10	$KClO_4$ 20 mM	0.037	0.046	0.125
A488-D10	KCl 20 mM	0.037	0.046	0.096
A488-D10	$KClO_4$ 40 mM	0.037	0.045	0.100
A488-D10	$KClO_4$ 60 mM	0.036	0.041	0.090
A488-D10	$KHCO_3$ 20 mM pH 7	0.039	0.040	0.076
A488-D10	$KHCO_3$ 20 mM pH 10	0.037	0.037	0.070
TMR-D10	H_2O	0.093	0.096	0.040
TMR-D10	$KHCO_3$ 20 mM pH 10	0.093	0.094	0
TMR-D10	TRIS 50 mM pH 7.5	0.092	0.092	0
FLU-D10	$KHCO_3$ 20 mM pH 10	0.044	0.046	0
FLU-D10	H_2O	0.047	0.049	0
FLU-D10	TRIS 50 mM pH 7.5	0.047	0.047	0

Table S7. Average anisotropy (*r*) for Rh110, A488, A488-D10, TMR-D10 and FLU-D10 in solution and in the hydrogel for different salt conditions.

S9. *Reference data*

Published experimental hydrodynamic radii for dextrans labelled with A488, TMR or fluorescein are compiled in Figure SI 5.

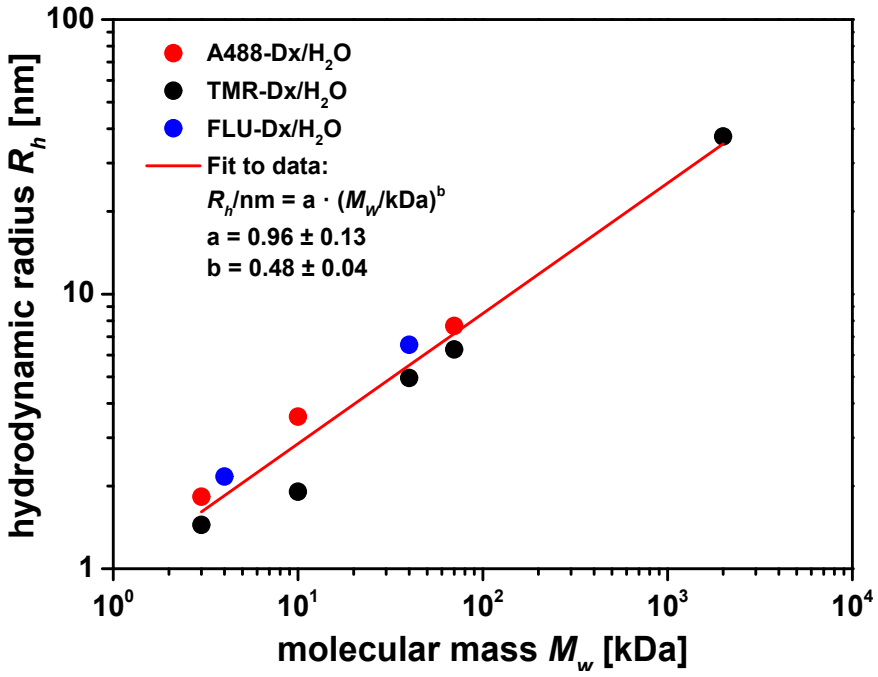

Figure S5. Fit of Flory scaling law to reference data for A488-D3 & A488-D10[8], A488-D70[9], TMR-Dx[10] and FLU-Dx[8]. R_h was taken as published or calculated via Stokes-Einstein equation. The systematic difference between TMR-Dx data (measured at 23 °C) and A488-Dx and Flu-Dx data (measured at 32 °C, except A488-D70 measured at 25 °C) is mainly attributed to calibration uncertainties. Reported temperature effects on R_h of dextrans in the relevant temperature and size range are about one order of magnitude smaller than the deviation of the two data sets and in the opposite direction: $-\Delta R_h/(R_h \Delta T) < 0.003\ \mathrm{K}^{-1}$ (extracted from Figure 1 in ref.[11]).

S10. *NMR Measurements*

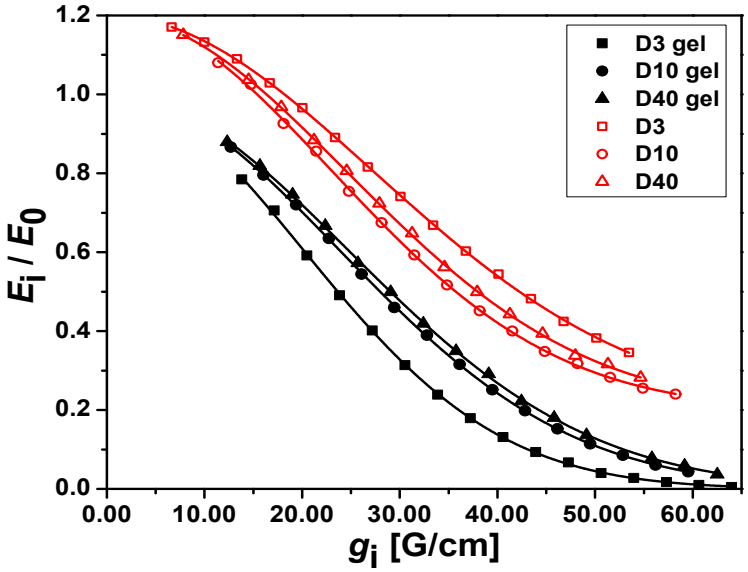

Figure S6. NMR data and fits for unlabelled dextrans (3 kDa, 10 kDa and 40 kDa) in hydrogels and in D_2O. Data was normalized and *xy* offset-corrected. For clarity reasons, the solution data (red) was vertically offset by 0.2.

The diffusion coefficients D were obtained by fitting the echo amplitudes (integral of the signals between 2.8 and 4.4 ppm) using Eq.7 (See main text). We performed several diffusion measurements with each sample, varying the key parameters δ and Δ_N and keeping constant the values of $\tau_N = 0.001$ s and γ=26752.22005 rad/s Gauss. Several combinations of Δ_N and δ were applied and the specific parameters are listed in the table S8.

	Solution			**Hydrogel**		
	δ [µs]	Δ_N [s]	D_{sol} [10^{-10}m^2/s]	δ [µs]	Δ_N [s]	D_{gel} [10^{-10}m^2/s]
D3	600	0.60	1.12	600	1.80	0.67
	800	0.30	1.15	700	1.40	0.65
	1000	0.10	1.16	800	1.00	0.68
D10	1000	0.30	0.97	750	1.70	0.30
	1200	0.25	0.96	1000	1.30	0.33
	1600	0.10	0.97	1500	0.50	0.31
D40	800	1.00	0.38	1200	1.60	0.096
	1000	0.80	0.38	1300	2.00	0.085
	1200	0.60	0.37	1400	1.80	0.096

Table S8. Parameters used for NMR measurements for unlabelled dextrans D3, D10 and D40. The fit provides the diffusion coefficient for each sample for the different experimental settings. The rows marked in yellow represent the curves shown in figure S6.

S11. *Technical details of the Brownian dynamics simulation*

General

In our Brownian dynamics simulation[12], we use a cubic simulation box with periodic boundary conditions containing 512 matrix particles and 1 tracer particle. About 200 independent simulation runs have been performed to generate typical trajectories for the statistical averages of the tracer's mean square displacements. The Brownian equations of motion were integrated with an Euler-algorithm. The time step Δt for the integration was chosen as $\Delta t < 2 \cdot 10^{-5}\ \tau_B$ (for model 1, 2 and 3a, TMR) and $\Delta t < 1.5 \cdot 10^{-6}\ \tau_B$ (for model 3b, TMR). $\tau_B = a^2 / D_0$ denotes the Brownian time. Here, a is the lattice constant of the matrix and D_0 the diffusion constant of the tracer particle in a pure solvent as obtained from the experiments. For FLU, Δt had to be chosen 10 times smaller. We carefully checked that the results for the statistical averages did not change upon further decreasing the time step such that the magnitude of Δt was small enough.

Simulation protocol

In our simulations we used the following protocol:

- Generation of the underlying gel structure:
  - The gel obstacles were placed on a simple cubic lattice of lattice constant a.
  - The matrix particles were randomly shifted up to half the lattice constant in each direction in model 2, 3a and 3b.
  - Springs were attached between the centers of neighboring matrix particles which were all undistorted, i.e. the rest lengths equaled exactly the corresponding particle separations.
- The tracer particle was placed in a void.
- The BD simulation was started and the system was equilibrated for a typical time of $t_{eq} >= 1\ \tau_B$.
- Statistics for the dynamical correlations was gathered by storing at least 100000 snapshots of the tracer trajectory $\vec{s}(t)$ at equidistant times within a sufficiently large time window of $t_{max} >= 40\tau_B$. In this time window, the tracer moved on average a distance of several lattice constants a.

Calculation of the hindrance factors

It was carefully checked that the long-time limit of the tracer's mean square displacement $\Delta s^2(t) = \left\langle \left(\vec{s}(t_0 + t) - \vec{s}(t_0)\right)^2 \right\rangle$ was reached. Here, <…> denotes the average over all $t_0 \in [0, t_{max} - t]$ and all independent simulation runs. The diffusion coefficient was obtained as $D = \lim_{t\to\infty} \frac{1}{6} \frac{d}{dt} \Delta s^2(t)$.[12, 13] As for an example, see Figure S7. We then performed a fitting procedure to describe the experimental hindrance factors $H=D/D_0$ as a function of R_h.

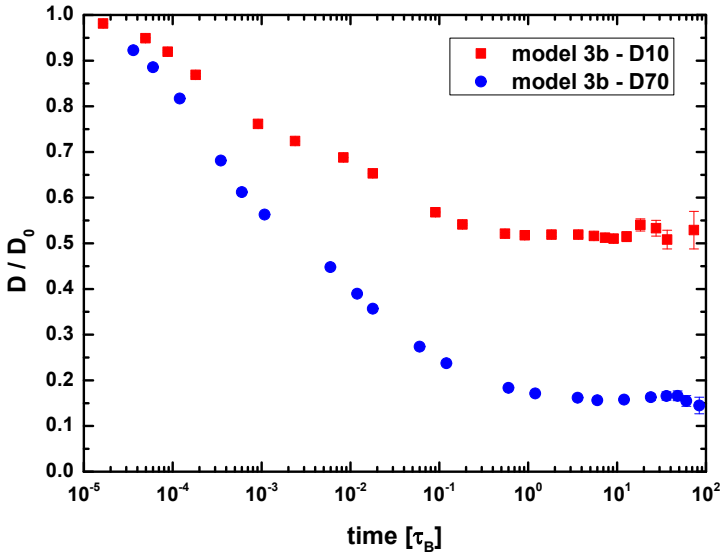

Figure S7. Hindrance factor D/D_0 versus time for two different tracers (D10 and D70) within model 3b. For very short times, the Diffusion coefficient approaches the Diffusion coefficient in solution D_0, as no collisions occur during these times. The long-time-limes is reached before 1 τ_B, as the diffusion coefficient does not decrease any further

Parameters

All model parameters were fixed according to Table S9 except the lattice constant a, which sets the pore size, and the obstacle radius R_{obst}, which was scaled with a factor such that the constraint of the experimentally prescribed volume fraction, φ, (measured by swelling analysis, see main text Sec.2.1.1) was fulfilled: $R_{obst} = \sqrt[3]{\frac{3\varphi}{4\pi}} a$. This leads to a coarse-grained obstacle radius comparable to the tracer size at least of the same order of magnitude. The additive diameters σ_{ij} used in Eq. (8), (10), (11) were therefore also fixed by $\sigma_{ij}=2\ R_{obst}$ for the obstacle-obstacle-interaction and $\sigma_{ij}=R_{obst} + R_h$ for the interaction between a matrix obstacle and a tracer of radius R_h. For the guest particle radii

R_h, we used our experimental values (see R_h in Table 3 in the results, 3.2.1). The short-time diffusivity of the obstacles was calculated via the Stokes-Einstein relation $D_{obst} = \frac{k_B T}{6\pi\eta R_{obst}}$. Here, η = 0.00095 Pa s is the viscosity of the solvent at T = 295 K (= 22 °C). We used ε_s=1 k_BT for the WCA-potential used in model 1, 2 and 3b. In model 3a, we used ε_G =12 k_BT since this value is above the value of 2 k_BT, which is found for self-avoiding polymers [14] but we expect our system to be stiffer. We have changed ε_G within the range of 4 k_BT and 20 k_BT and did not obtain an improved fit to the experimental data.

In conclusion, out of the 12 parameters shown in Table S9, 9 are fixed by physical constraints, namely the obstacle radius R_{obst}, and consequently also the obstacle self-diffusion constant D_{obst} and the additive diameters $\sigma_{obst,\ obst}$, $\sigma_{obst,\ D0}$, $\sigma_{obst,\ D3}$, $\sigma_{obst,\ D10}$, $\sigma_{obst,\ D40}$, $\sigma_{obst,\ D70}$, $\sigma_{obst,\ D500}$. Hence only 3 parameters are left: The lattice constant a, the spring constant k and the interaction parameters ε_s, resp. ε_G, (plus possibly the parameter ε_a in model 3b). ε_a and a are real fit parameters. We have checked that a change of k and the interaction parameters ε_s, resp. ε_G give indifferent fit quality.

Fitting and conclusion

For the fixed choice of a, the whole hindrance factors H were simulated as a function of R_h, i.e. for all tracer radii used in the experiments. These sets of simulation data were compared to the experimental data and an optimal value of a was obtained by the best fit. For model 3b, two fit parameters were used, namely the lattice constant a and the attraction strength ε_a. This results in better fitting in particular for small R_h. We remark here that the attraction was essential. In a purely repulsive dextran-matrix interaction model, a second fit parameter would not give a significant improvement of the fit. Additional simulations performed within model 3b using a Gaussian softened core showed a similar fit quality as that with a WCA-core such that we conclude that the attraction itself rather than the details of the repulsion is crucial to describe the experimental data properly.

Dye	Model	initial gel simple cubic lattice constant [10^{-9}m]	obstacle radius [10^{-9}m]	obstacle self diffusion constant [10^{-11}m^2/s]	spring constant [10^{-4}N/m]	Matrix-dextran-interaction parameters (at T=20 °C) [10^{-20}J]	$\sigma_{obst,obst}$ [10^{-9}m]	$\sigma_{obst,D0}$ [10^{-9}m]	$\sigma_{obst,D3}$ [10^{-9}m]	$\sigma_{obst,D10}$ [10^{-9}m]	$\sigma_{obst,D40}$ [10^{-9}m]	$\sigma_{obst,D70}$ [10^{-9}m]	$\sigma_{obst,D500}$ [10^{-9}m]
TMR	1	11.75	2.48	0	inf	$\varepsilon_s = 1k_BT \approx 0.405$	4.95	3.03	4.19	5.55	8.48	10.34	
	2	11.75	2.48	9.18	6.17	$\varepsilon_s = 1k_BT \approx 0.405$	4.95	3.03	4.19	5.55	8.48	10.34	
	3a	10.03	2.11	10.77	6.17	$\varepsilon_G = 12k_BT \approx 4.86$	4.23	2.66	3.82	5.18	8.11	9.97	
	3b	14.35	3.02	7.52	6.17	$\varepsilon_s = 1k_BT \approx 0.405$ $\varepsilon_a = 3k_BT \approx 1.21$	6.05	3.57	4.73	6.09	9.02	10.88	
FLU	1	31.73	4.86	0	inf	$\varepsilon_s = 1k_BT \approx 0.405$	9.73	5.41	6.57	7.93	10.86		25.16
	2	31.73	4.86	4.68	6.17	$\varepsilon_s = 1k_BT \approx 0.405$	9.73	5.41	6.57	7.93	10.86		25.16
	3a	30.29	4.64	4.90	6.17	$\varepsilon_G = 12k_BT \approx 4.86$	9.29	5.19	6.35	7.71	10.64		24.94
	3b	44.71	6.85	3.32	6.17	$\varepsilon_s = 1k_BT \approx 0.405$ $\varepsilon_a = 3k_BT \approx 1.21$	13.71	7.40	8.56	9.92	12.85		27.15

	D0	D3	D10	D40	D70	D500
radius [10^{-9}m]	0.55	1.7	3.1	6.0	7.9	20

Table S9. Parameters used for Brownian dynamics simulations for model 1 (fixed gel matrix, steric interaction), model 2 (flexible gel matrix, steric interaction), model 3a (flexible gel matrix, soft interaction), model 3b (flexible gel matrix, steric interaction and attractive shell).

References

1. D. Magde, R. Wong and P. G. Seybold, *Photochem. Photobiol.*, 2002, **75**, 327-334.
2. X.-F. Zhang, Y. Zhang and L. Liu, *J. Lumin.*, 2014, **145**, 448-453.
3. N. L. Thompson, in *Topics in Fluorescence Spectroscopy*, ed. J. R. Lakowicz, Plenum Press, New York, 1991, vol. 1, pp. 337-378.
4. J. Stejskal and J. Horská, *Makromol. Chem.*, 1982, **183**, 2527-2535.
5. *Release on the Refractive Index of Ordinary Water Substance as a Function of Wavelength, Temperature and Pressure*, The International Association for the Properties of Water and Steam, Erlangen, Germany, 1997.
6. D. Toptygin, *J. Fluoresc.*, 2003, **13**, 201-219.
7. E. Banachowicz, A. Patkowski, G. Meier, K. Klamecka and J. Gapinski, *Langmuir*, 2014, **30**, 8945-8955.
8. T. Kihara, J. Ito and J. Miyake, *PLoS One*, 2013, **8**, e82382.
9. S. Lehmann, S. Seiffert and W. Richtering, *J. Am. Chem. Soc.*, 2012, **134**, 15963-15969.
10. Z. Zhang, E. Nadezhina and K. J. Wilkinson, *Antimicrob. Agents Chemother.*, 2011, **55**, 1075-1081.
11. M. A. Masuelli, *J. Polym. Biopolym. Phys. Chem.*, 2013, **1**, 13-21.
12. M. P. Allen and D. J. Tildesley, *Computer Simulation of Liquids (Oxford Science Publications)*, Oxford University Press, 1989.
13. B. J. Alder, D. M. Gass and T. E. Wainwright, *J. Chem. Phys*, 1970, **53**, 3813-3826.
14. A. A. Louis, P. G. Bolhuis, E. J. Meijer and J. P. Hansen, *J. Chem. Phys*, 2002, **117**, 1893-1907.